

Published in International Journal of Thermal Sciences
2007
This is author version post-print
Archived in Dspace@nitr <http://dspace.nitrkl.ac.in/dspace>

**Numerical Study of Laminar Free Convection About a Horizontal Cylinder with
Longitudinal Fins of Finite Thickness**

S.C. Haldar*, G.S. Kochhar and K. Manohar
Department of Mechanical and Manufacturing Engineering
Faculty of Engineering
University of the West Indies, St. Augustine, Trinidad
Trinidad and Tobago, West Indies

R.K. Sahoo
Department of Mechanical Engineering
National Institute of Technology, Rourkela, India

Abstract

Conjugate numerical solution of laminar free convection about a horizontal cylinder with external longitudinal fins of finite thickness has been carried out. Fins alone contribute very small to the total heat transfer but they greatly influence the heat transfer from the uncovered area of the cylinder. Among the various fin parameters, thickness has the greatest influence on heat transfer. The rate of heat transfer is above that for the free cylinder only when the attached fins are very thin. For thin fins, there exist a fin length, which maximizes the rate of heat transfer. The optimum number and dimensionless length of the fins were obtained as 6 and 0.2 respectively when fin thickness is 0.01, the thinnest among those investigated in this study.

Keywords : Free convection, Longitudinal fin, Horizontal cylinder

*Corresponding author
on lien from NIT, Rourkela, India
E-mail : schaldar@rediffmail.com

1. Introduction

Free convection about a horizontal cylinder is a relatively old topic and has been investigated extensively by analytical, numerical and experimental techniques. The three relatively recent papers by Wang et al [1,2] and Saito et al [3] provide a comprehensive list of articles on this topic and those are not cited here to avoid repetition. In order to enhance the rate of heat transfer from the cylinder, the fins are attached to it, most commonly in longitudinal or radial orientation having uniform thickness. Depending on the applications, the fins may be fixed on the inner or the outer surface of a cylinder. In case of radial fins of uniform thickness attached to a circular cylinder, each fin surface is parallel to one of the planes of a cylindrical polar co-ordinates and this renders the discretisation of the physical domain easier. But this is not so for the longitudinal fins of uniform thickness fixed on to a circular cylinder. The recent articles, which the authors could locate, on convection from horizontal cylinder with longitudinal fins are by Rustum and Soliman [4], Chai and Patankar [5] dealing with internal fins and by Bassam [6,7] and Halder [8] dealing with external fins. All these articles [4-8] suffer from two major drawbacks, the assumption of isothermal fins at the base value and negligible fin thickness. In order to take advantage of the fin surfaces coinciding with the radial co-ordinate direction of cylindrical polar co-ordinate, the fin thickness was neglected. When the fin thickness is assumed zero, the temperature variation along the fins cannot be determined numerically and this necessitates another assumption of uniform fin temperature at the base value. These two assumptions render the problem far removed from the actual. In fact, this study shows that reduction in fin thickness results greater variation in temperature from the base to the tip of the fins. Thus the two assumptions, isothermal fins at the base temperature and the negligible fin thickness, are not compatible to each other. Elimination of these two assumptions has the potential to yield results very much different from those reported previously. With the inclusion of fin thickness, the results now depend on two additional parameters, the fin thickness itself and the fin thermal conductivity.

2. Problem description

Fig.1 presents the schematic of the problem under consideration along with the chosen coordinate system and the respective velocity components. The direction of

gravitational acceleration has been indicated in the figure. The problem is symmetric about the vertical diameter, the upper and lower segments of which correspond to $\theta=0$ and 180° respectively. The fins are rectangular having a thickness t and length L , and are positioned at an equal angular spacing around the horizontal cylinder. The cylinder surface was considered isothermal.

3. Governing equations and boundary conditions

The physical domain includes two different matter states; the solid fins on the cylinder and the fluid around it. For the former, only the conduction equation needs to be solved. The root and the tip of each fin were assumed straight rendering the cross-sectional geometry of the fins as rectangular. Accordingly, the Cartesian co-ordinates were adopted for the fins and the equation to be solved is

$$\frac{\partial^2 T}{\partial x^2} + \frac{\partial^2 T}{\partial y^2} = 0 \quad ..(1)$$

Where x is the co-ordinate distance along the length of each fin and y along its thickness.

In order to solve the equation, temperature conditions need to be specified on the four boundary surfaces of each fin and these are

$T=1.0$ at the base

$$k_f \frac{\partial T}{\partial y} = k_a \frac{1}{r} \frac{\partial T}{\partial \theta} \quad \text{at the upper surfaces} \quad ..(1a)$$

$$k_f \frac{\partial T}{\partial y} = -k_a \frac{1}{r} \frac{\partial T}{\partial \theta} \quad \text{at the lower surfaces and} \quad ..(1b)$$

$$k_f \frac{\partial T}{\partial x} = k_a \frac{\partial T}{\partial r} \quad \text{at the fin tips} \quad ..(1c)$$

For the fluid region, the governing equations in vorticity stream-function formulation with Boussinesq's approximation are, though well known, written below for the sake of completeness.

$$\text{Vorticity transport : } u \frac{\partial \Omega}{\partial r} + \frac{v}{r} \frac{\partial \Omega}{\partial \theta} = \nabla^2 \Omega + Gr \left[\sin \theta \frac{\partial T}{\partial r} + \frac{\cos \theta}{r} \frac{\partial T}{\partial \theta} \right] \quad ..(2)$$

$$\text{Stream-function : } \nabla^2 \psi = -\Omega \quad ..(3)$$

$$\text{Energy : } u \frac{\partial T}{\partial r} + \frac{v}{r} \frac{\partial T}{\partial \theta} = \frac{1}{Pr} \nabla^2 T \quad ..(4)$$

Where the operator $\nabla^2 = \frac{\partial^2}{\partial r^2} + \frac{1}{r} \frac{\partial}{\partial r} + \frac{1}{r^2} \frac{\partial}{\partial \theta^2}$

The stream-function and the two velocity components are related by

$$u = \frac{1}{r} \frac{\partial \psi}{\partial \theta} \quad \text{and} \quad v = -\frac{\partial \psi}{\partial r} \quad \dots(5)$$

The symmetry about the vertical diameter was taken advantage of and the governing equations were solved in one half of the finned cylinder. A pseudo cylinder in the far field was considered as one of the boundaries to facilitate computation. Accordingly, the computational domain is bounded by the cylinder surface with the fins attached to it, the upper vertical, the outer pseudo cylinder and the lower vertical symmetry line. The diameter of the pseudo cylinder was chosen large enough not to influence the results of the numerical solution. The fluid was deemed to cross the outer pseudo cylinder orthogonally. The boundary conditions for the fluid region are then stated below.

$$\text{Cylinder : } \psi = 0, \quad \Omega = -\frac{\partial^2 \psi}{\partial r^2} \quad \text{and} \quad T=1.0$$

Fin surfaces : $\psi = 0$ at all the surfaces of each fin. The upper and lower surfaces of each fin were assumed to coincide with the constant θ -line passing through the center of the respective fins for the purpose of determining the vorticity values at these surfaces.

$$\text{Accordingly, } \Omega = -\frac{1}{r^2} \frac{\partial^2 \psi}{\partial \theta^2} \quad \text{at the upper surfaces, } \Omega = \frac{1}{r^2} \frac{\partial^2 \psi}{\partial \theta^2} \quad \text{at the lower surfaces and}$$

$$\Omega = -\frac{\partial^2 \psi}{\partial r^2} \quad \text{at the tips of each fin.}$$

The boundary conditions on temperature at the three surfaces of each fin have been stated in equations (1a), (b) and (c).

$$\text{Symmetry lines at } \theta=0 \text{ and } \pi : \psi = 0 \quad \text{with} \quad \frac{\partial^2 \psi}{\partial \theta^2} = 0 \quad \text{as the additional condition on } \psi .$$

$$\text{Symmetry about } \theta \text{ demands } v=0 \text{ and } \frac{\partial u}{\partial \theta} = 0, \text{ resulting to } \Omega = \frac{\partial v}{\partial r} - \frac{1}{r} \frac{\partial u}{\partial \theta} = 0 . \text{ Also,}$$

$$\text{symmetry requires } \frac{\partial T}{\partial \theta} = 0 \quad \text{as the condition on temperature.}$$

Outer pseudo cylinder : The assumption that the fluid enters and leaves the computational domain with radial velocity only yields $v = \frac{\partial \psi}{\partial r} = \frac{\partial^2 \psi}{\partial r^2} = 0$. Upon substitution, eqn.(3)

reduces to $\Omega = -\frac{1}{r^2} \frac{\partial^2 \psi}{\partial \theta^2}$.

The temperature boundary conditions of the incoming and outgoing fluids need to be specified separately and these are $T=0$ if u is $-ve$ (inflow) and $\partial T/\partial r=0$ if u is $+ve$ (outflow).

It may be mentioned here that Farouk and Guceri [9,10] assumed $\partial T/\partial r=0$ throughout the outer boundary. Kuehn and Goldstein[11] and Bassam [6,7] in his two articles had set a priori the outflow-inflow interface at 30° away from the upper vertical symmetry line. It has been reported in Haldar [8] that the location of outflow-inflow interface varies from 30° at $Gr=10^2$ to about 20° at $Gr=10^6$ and these values remain almost unchanged by the presence of fins on the cylinder.

4. Numerical Method

The governing dimensionless equations were solved by finite difference technique based on control volume discretization over non-staggered grids. The equations were discretized following the cell average QUICK scheme proposed by Leonard [12] which is expected to produce grid-independent results with fewer grids [13] in comparison to second order upwinding. However, central differencing was employed for the wall adjacent control volumes.

The program was solved with various pairs of radial and angular grid spacing in order to arrive at suitable values producing grid-independent results. The value of radial grid spacing adjacent to the cylinder than that further away has strong influence on the results. Initially radial spacing was gradually reduced keeping the angular spacing fixed. This exercise yielded a spacing of 0.025 up to a radial distance of fin tip plus 0.25, and 0.075 further away as sufficient. The angular spacing was then varied and a uniform value of 2° was found to produce results within acceptable accuracy. Each fin was discretised by 200 grids along the fin length and 20 along its thickness.

Solution was initiated with dimensionless temperature as zero everywhere within the computational domain except the cylinder surface and the base of the fins.

Equation(1) was solved to obtain the temperature distributions in each fin which were then substituted in the discretised form of equations(1a), (b), and (c) to update the temperatures at the boundaries of each fin. Equation(4) was then solved for temperature, eqn.(2) for vorticity, and eqn.(3) for stream-function values in the fluid region. Boundary vorticity values were updated and the cycle was repeated till a converged solution was obtained.

Individual equations were converged to 0.0001%. While the global convergence was considered achieved when the differences of vorticity values at each grid point between two consecutive iteration cycles were less than 0.001% where one iteration cycle includes solution of eqn.(1) to (4).

Position of the far-field pseudo-cylinder was found to have almost no effect on the results if it is located beyond 4.5 times the radius of the cylinder, measured from the center. However, the solutions were carried out for an outer cylinder radius of 6.75.

5. Results and discussions

The results were first generated for the case of plain cylinder for various Gr values and Nusselt numbers obtained were found to differ by less than 2% with those reported by Saitoh et al [3]. For the case of finned cylinder, the rate of heat transfer depends on the number, length, thickness and thermal conductivity of the fins, and also on Grashof number. In order to reduce the computation time and to keep the length of the paper within reasonable limit, the solution was carried out for a fixed Gr value of 10^5 . The discussions will mainly focus on the effects of different fin parameters on the rate of heat transfer from the finned cylinder. Results were generated for the $0 \leq N \leq 18$ equally spaced over the entire(360°) cylinder, $0.1 \leq L \leq 0.6$, $0.01 \leq t \leq 0.05$ and the fin to air thermal conductivity ratio, k_f/k_a of 2000 and 16000. The fluid surrounding the cylinder was chosen as air by specifying a Pr value of 0.7.

5.1 Effect of fin parameters

Rate of heat transfer from a finned cylinder consists of two components; one from the cylinder surface and the other from the three surfaces of each fin. Both these components are influenced by the various fin parameters viz. fin thickness, length, number of fins and thermal conductivity.

Contribution to heat transfer by the fins and its variation with fin thickness and number of fins will be studied first. From the fin base, heat is conducted to the fin and then convected from the fin surfaces to the air around the fins. Increase in fin thickness offers greater resistance to conduction and as a consequence, the temperature at any location in the fin greatly increases with fin thickness. In order to corroborate this, the temperature variation along x-axis at the center of the fin positioned at $\theta=60^\circ$ has been plotted in fig.2 against the radial distance for five values of fin thickness. All the five profiles are for 18 fins of dimensionless length 0.4 spaced equally over the entire cylinder. This increase in fin temperature reduces the temperature gradient at the fin base for a fixed cylinder surface temperature, which may be noted at $r=1$ in fig.2, and on the contrary, the base area increases with fin thickness. The consequence of these two effects is that the rate of heat transfer conducted to a fin significantly decreases with increase in thickness beyond a dimensionless value of about 0.02, fig.3. However, this reduction has marginal effect on the total heat transfer rate since the contribution to it by the fins is much smaller than that by the cylinder surface. As expected, the contribution from the fins increases when the cylinder is provided with more fins of same thickness.

Next, the contribution to heat transfer by the cylinder surface will be discussed. For a fixed temperature of the cylinder surface, the temperature of air adjacent to the finned cylinder is determined by the temperature of the fin surfaces. Accordingly, the increase in fin temperature due to increase in thickness, fig.2, causes the air temperature adjacent to the fins and the cylinder to rise. This may be noted from fig.4 presenting the variation of air temperature at $\theta=90^\circ$ as a function of radial distance and fin thickness for 18 fins of length 0.4. At a radial distance of 1.2, the air temperature increases from about 0.2 to approximately 0.6 when the fin thickness increases from 0.01 to 0.05. This in turn reduces the temperature gradient and hence the rate of heat transfer from the cylinder surface, fig.5. It also reveals that the dimensionless rate of heat transfer from the cylinder is less for more fins of same length and thickness. This is again due to increased air temperature adjacent to the cylinder and a consequent decrease in temperature gradient at the cylinder surface caused by more number of fins. Another alarming observation from fig.5 is that the fins reduce the heat transfer below its value for the plain cylinder(no fin) for most of the ranges of the fin parameters covered in this study. It may be appropriate

to mention here that a similar trend has been reported by Tolpadi and Kuehn[14] for annular fins around circular cylinder.

Figures 6 and 7 have been presented in order to study the influence of fin length on heat transfer from the fins and that from the cylinder surface respectively. Contribution to heat transfer by the fins increases with fin length for all the five thickness values investigated. The profile for $t=0.01$ reaches maximum at a fin length of approximately 0.2, fig.6. However, it may be recalled here that a major fraction of the total heat transfer is due to cylinder surface. The case of cylinder without fins has also been shown in fig.7 for reference. Attaching fins increases heat transfer over that of the free cylinder only for the case of $t=0.01$, the thinnest of the five cases studied.

For the chosen thickness of 0.01, the variation of total heat transfer with length and number of fins may be noted from fig.8. The sharp increase in heat transfer up to a length of 0.2 and marginal changes with further increase in length hold good for all the three profiles. There exists a fin length at which the rate of heat transfer is maximum and this length increases as the number of fins reduces. If 0.2 is taken as the preferred fin length, fig.8 also shows that the number of fins has marginal effect on the heat transfer at the chosen fin length. When the cost of fins is into consideration, the optimum number of fins may safely be taken as 6.

The numerical solution requires the value of fin to air thermal conductivity ratio as an input. The results presented above are for a value of 2000. In order to study the influence of fin thermal conductivity, the results were also generated for a fin to air thermal conductivity ratio of 16000. Fig.9 presents the heat transfer ratio for the two components of heat transfer as a function of fin thickness. The near horizontal profile of the main component, the one from the cylinder surface, implies that the influence of fin for free convection around horizontal cylinder remains almost unchanged when the fin thermal conductivity was varied eight times.

It will be interesting to note that for isothermal fins at the base temperature with negligible thickness, the rate of heat transfer is greater than that for the free cylinder for any number of fins of any length [6,8].

5.2 Flow pattern

Buoyancy generates fluid motion around the cylinder in the (r,θ) plane with radial and tangential velocity components. The figures 10 and 11 plot the radial and tangential velocity components respectively as a function of radial distance at $\theta=90^\circ$ for 18 equally spaced fins of dimensionless length 0.4. The five profiles in each figure correspond five different fin thickness values. The fins are located at 20° apart from $\theta=0^\circ$ and accordingly no fin exists at the chosen angular location of 90° . For the sake of presentation, the dimensionless radial distance has been limited to 2.0 though the computational domain extends to a value of 6.75. These plots reveal two important facts that the magnitudes of velocity vary appreciably with fin thickness but the nature of the profiles remain similar. The qualitative nature of the streamlines around the cylinder were found similar to those reported for negligible fin thickness [8], and were also observed to vary little with fin thickness. For these reasons, the plots of streamlines have been shown only for the case of 12 fins of dimensionless length 0.2 and thickness 0.01, fig.12. The fluid is drawn towards the heated cylinder over a large angular area. The flow gradually converges as it approaches the cylinder and then rises along its periphery and finally moves out through a narrow nearly vertical region, ordinarily called plume. The presence of fins causes the fluid to take a tortuous path adjacent to the cylinder.

The negative values of tangential velocity, fig.11, are due to the rising air around the cylinder identified by decreasing θ direction. It may be noted from the two figures that the tangential components are much larger than the radial ones because the fluid adjacent to the cylinder rises almost vertically at the chosen angular position of $\theta=90^\circ$.

The fin temperature increases with fin thickness, fig.2, for a fixed temperature of the cylinder surface. This in turn increases the temperature averaged over the solid surfaces consisting of the cylinder and the fins. This increased temperature difference between the solid surface and the far stream ambient inducts more air to flow over the heated surface, which explains the increase in radial and tangential velocity components with fin thickness.

6. Conclusions

Conjugate numerical solution of laminar free convection about a horizontal cylinder with external longitudinal fins of finite thickness has been reported in this

article. The fins themselves contribute very little to the total heat transfer but their presence greatly alter the fluid temperature adjacent to the cylinder surface and consequently the heat transfer from the uncovered area of the cylinder. Among the various fin parameters, thickness plays the most influential role in determining the performance of the fins, which has not been considered in most of the studies reported previously. The effect of fins on heat transfer from the cylinder was found negative except for very thin fins. For thin fins, there exist a fin length, dependent of the number of fins, at which the rate of heat transfer is maximum. The thermal conductivity of fins was found to have little effect on heat transfer. For the thinnest fin of 0.01 of all the five thickness values investigated, the optimum number and length of the fins were found as 6 and 0.2 respectively.

Nomenclature

g	acceleration due to gravity, $m.s^{-2}$
Gr	Grashof number, $Gr = g\beta(T_c^* - T_\infty^*)r_c^{*3} / \nu^2$
k_a	thermal conductivity of air, $W.m^{-1}.K^{-1}$
k_f	thermal conductivity of fin, $W.m^{-1}.K^{-1}$
L^*	fin length, m; $L = L^* / r_c^*$
N	number of fins over the entire cylinder
Pr	Prandtl number
r^*	radial distance, m; $r = r^* / r_c^*$
r_c^*	cylinder radius, m; $r_c = 1.0$
t^*	fin thickness, m; $t = t^* / r_c^*$
T^*	temperature, K; $T = (T^* - T_\infty^*) / (T_c^* - T_\infty^*)$
T_c^*	cylinder surface temperature, K; $T_c = (T_c^* - T_\infty^*) / (T_c^* - T_\infty^*) = 1.0$
T_∞^*	free stream temperature, K; $T_\infty = (T_\infty^* - T_\infty^*) / (T_c^* - T_\infty^*) = 0.0$
u^*	radial velocity, $m.s^{-1}$; $u = u^* / (\nu / r_c^*)$
v^*	angular velocity, $m.s^{-1}$; $v = v^* / (\nu / r_c^*)$
x^*	distance along fin length, m; eqn.(1); $x = x^* / r_c^*$
y^*	distance along fin thickness, m; eqn.(1); $y = y^* / r_c^*$

Greek symbols

β	volumetric coefficient of thermal expansion, K^{-1}
ν	kinematic viscosity, $m^2.s^{-1}$
θ	angular coordinate

ψ stream-function, $\text{m}^2 \cdot \text{s}^{-1}$; $\psi^* = \psi / g$

Ω vorticity about z-axis, s^{-1} ; $\Omega^* = \Omega / (g / r_c^2)$

Superscript

* dimensional quantity

References

- [1] P. Wang, R. Kahawita and D. L. Nguyen, Numerical computation of the natural convection flow about a horizontal cylinder using splines, *Numerical Heat Transfer, Part A* 17 (1990) 191-215.
- [2] P. Wang, R. Kahawita and D. L. Nguyen, Transient laminar natural convection from horizontal cylinders, *Int. J. Heat Mass Transfer* 34 (1991) 1429-1442.
- [3] T. Saitoh, T. Sajiki and K. Muruhara, Bench mark solutions to natural convection heat transfer problem around a horizontal circular cylinder, *Int. J. Heat Mass Transfer* 36 (5) (1993) 1251-1259.
- [4] I. M. Rustum and H. M. Soliman, Numerical analysis of laminar mixed convection in horizontal internally finned tubes, *Int. J. Heat Mass Transfer* 33 (7) (1990) 1485-1496.
- [5] J. C. Chai and S. V. Patankar, Laminar natural convection in internally finned horizontal annuli, *Numerical Heat Transfer, Part A* 24 (1993) 67-87.
- [6] A. H. Bassam, Optimization of natural convection heat transfer from a cylinder with high conductivity fins, *Numerical Heat Transfer, Part A* 43 (2003) 65-82.
- [7] A. H. Bassam, Natural convection heat transfer from a cylinder with high conductivity permeable fins, *J. Heat Transfer, ASME Trans.* 125 (2003) 282-288.
- [8] S. C. Haldar, Laminar free convection around a horizontal cylinder with external longitudinal fins, *Heat Transfer Engineering* 25(6) (2004) 45-53.
- [9] B. Farouk and S. I. Guceri, Natural convection from a horizontal cylinder-laminar regime, *J. Heat Transfer, ASME Trans.* 103 (1981) 522-527.
- [10] B. Farouk and S. I. Guceri, Natural convection from a horizontal cylinder-turbulent regime, *J. Heat Transfer, ASME Trans.* 104 (1982) 228-235.
- [11] T. H. Kuehn and R. J. Goldstein, Numerical solution to the Navier-Stokes equations for laminar natural convection about a horizontal isothermal circular cylinder, *Int. J. Heat Mass Transfer* 23 (1980) 971-979.
- [12] B. P. Leonard, Bounded higher-order upwind multidimensional finite-volume convection-diffusion algorithms, *Adv. in Heat Transfer* edited by W.J. Minkowycz and E. M. Sparrow.

- [13] A. Sharma and V. Eswaran, Conservative and consistent implementation and systematic comparison of SOU and QUICK schemes for recirculating flow computation on a non-staggered grid, Proc. 2nd Int. and 29th National FMEP conf., Roorkee, India (2002) 351-358.
- [14] A. K. Tolpadi and T. H. Kuehn, Computation of conjugate three-dimensional natural convection heat transfer from a transversely finned horizontal cylinder, Numerical Heat Transfer, Part A 16 (1989) 1-13.

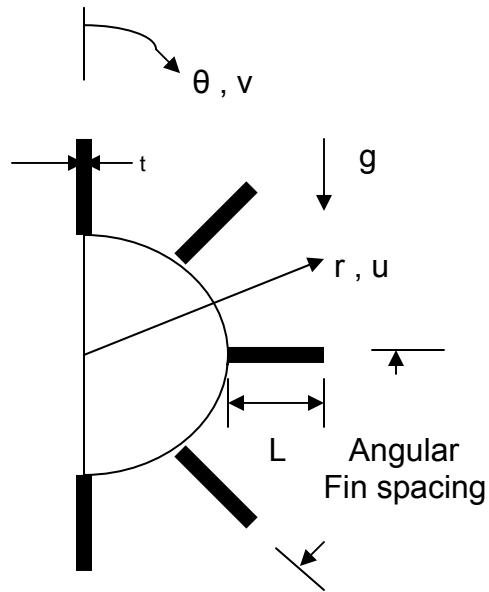


Fig.1 Schematic of the physical problem

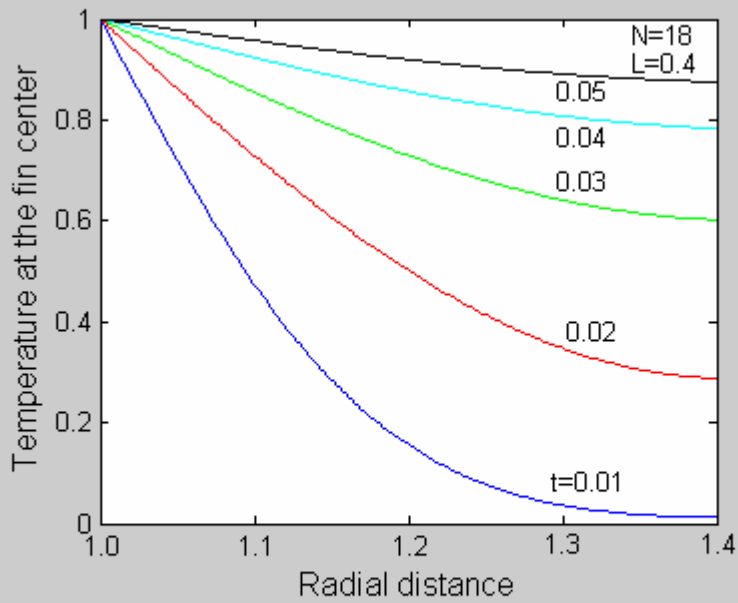


Fig.2 Effect of fin thickness on the fin temperature for the fin located at 60 degree

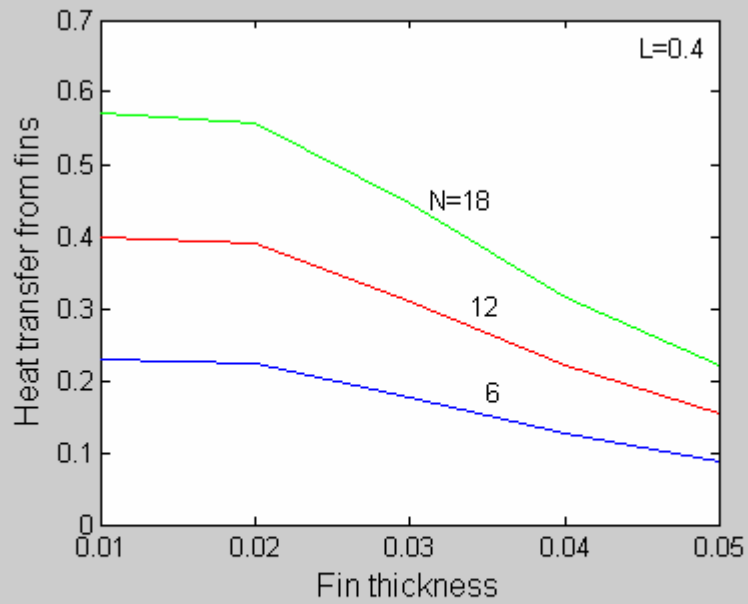


Fig.3 Variation of heat transfer from the fins with fin thickness and number of fins

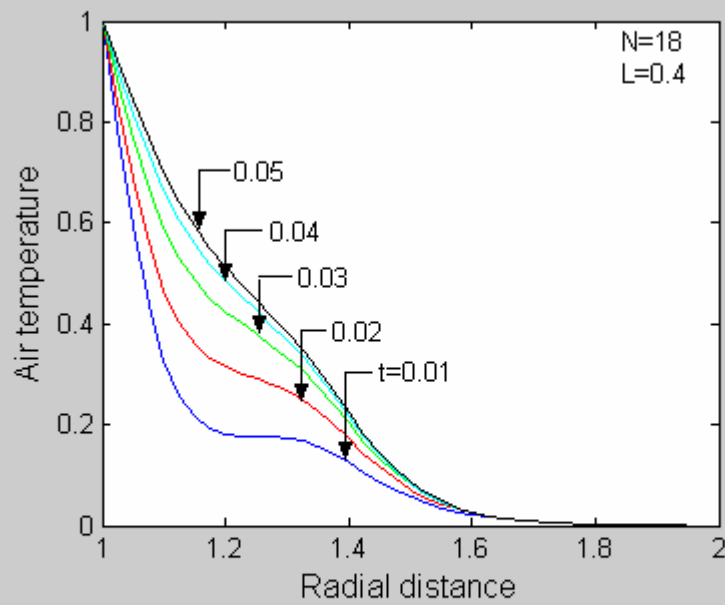


Fig.4 Effect of fin thickness on fluid temperature at 90 degree

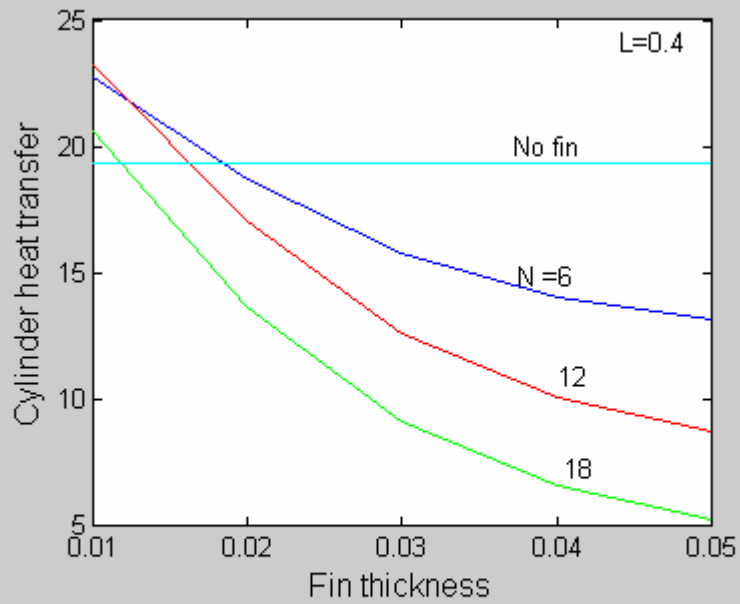


Fig.5 Variation of heat transfer from the uncovered part of the cylinder with fin thickness and number of fins

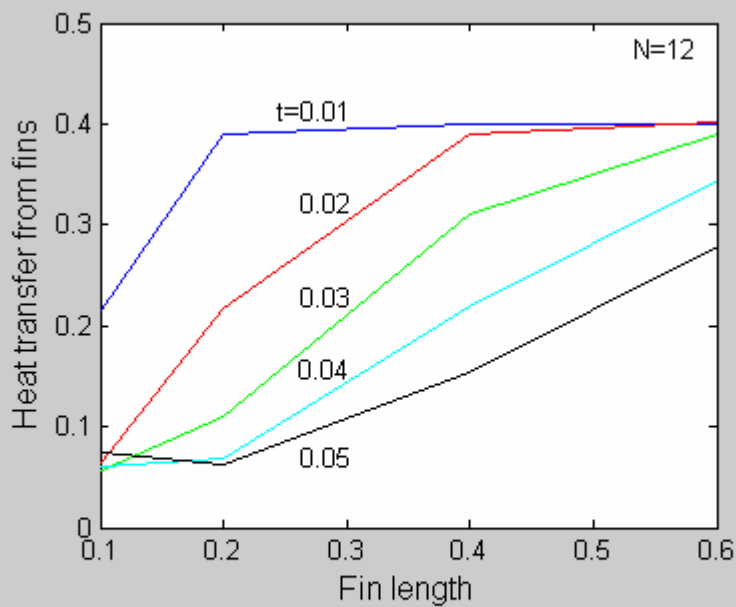


Fig.6 Variation of heat transfer from the fins with fin length and fin thickness

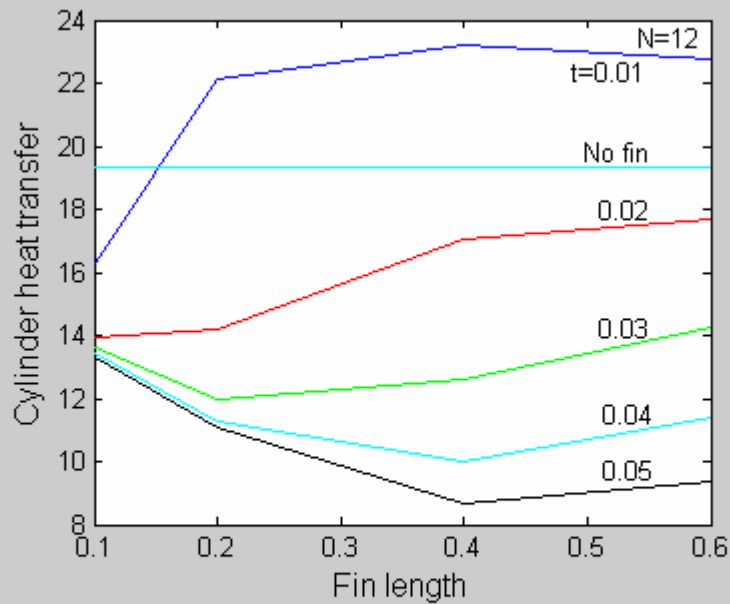


Fig.7 Variation of heat transfer from the uncovered part of the cylinder with fin length and fin thickness

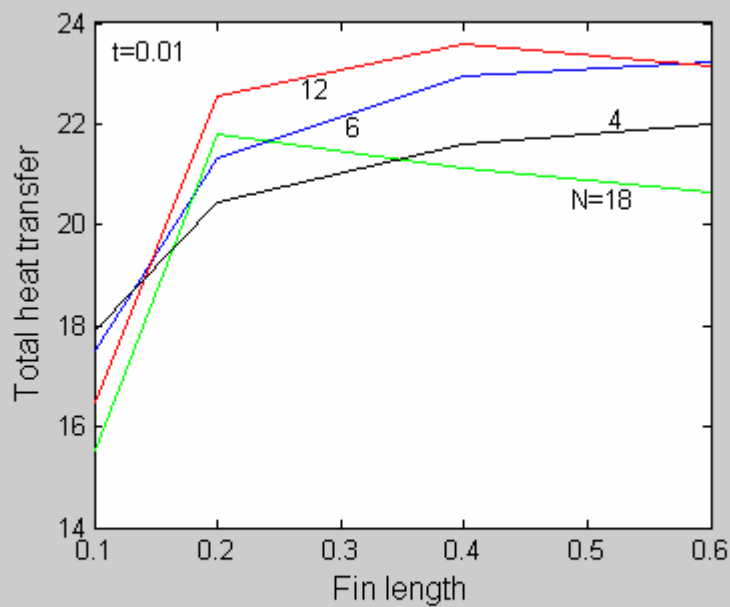


Fig.8 Effects of fin length and number of fins on total heat transfer for fins of thickness 0.01

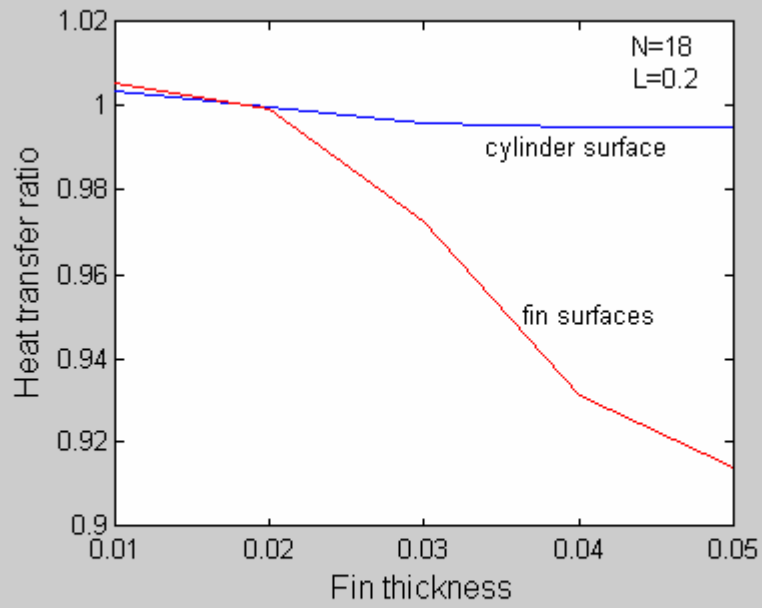


Fig.9 Ratio of heat transfer for fin to air thermal conductivity 16000 to that for 2000

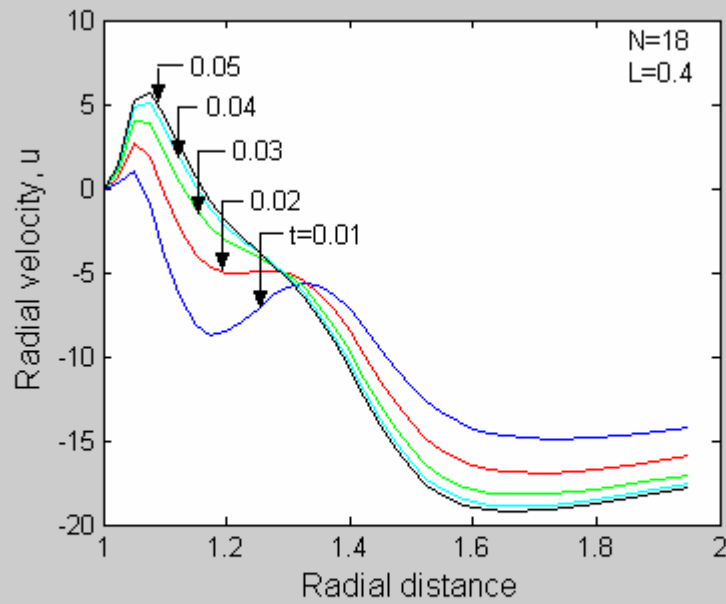


Fig.10 Effect of fin thickness on radial velocity at 90 degree

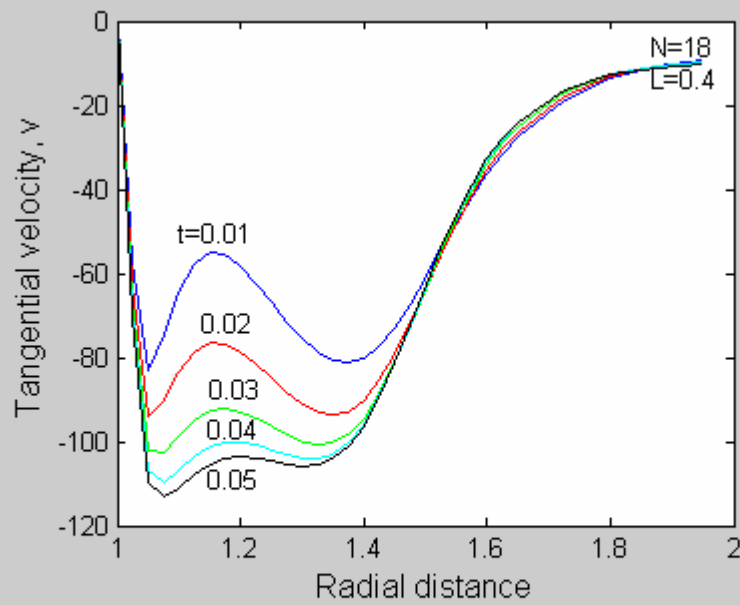


Fig.11 Effect of fin thickness on tangential velocity at 90 degree

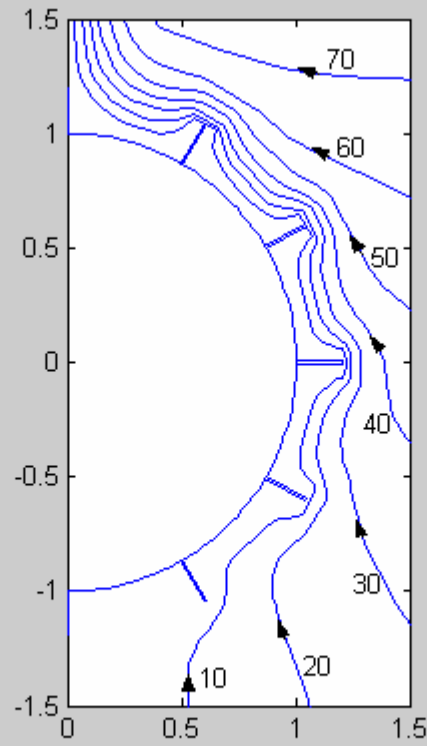


Fig.12 Streamlines for 12 fins of dimensionless length 0.2, thickness 0.01